

## Organic Radicals As Spin Filters

Carmen Herrmann,\* Gemma C. Solomon,\* and Mark A. Ratner

Department of Chemistry, Northwestern University, Evanston, Illinois 60208

Received December 11, 2009; E-mail: c-herrmann@northwestern.edu; g-solomon@northwestern.edu

With the trend toward miniaturization, the notion of molecules as building blocks in electronic devices<sup>1</sup> has gained increasing popularity since its introduction in 1974.<sup>2</sup> Over the past decade, molecular electronics has been combined with spintronics,<sup>3</sup> often employing nonmagnetic molecular bridges with magnetism introduced to the system via ferromagnetic electrodes or via circularly polarized light.<sup>4</sup> Another experimental approach to molecular spintronics is a magnetic molecule between, in general, nonmagnetic probes. These magnetic bridges typically contain metal atoms,<sup>5</sup> but recently, organic radicals have been investigated in gold nanoarrays<sup>6</sup> as well as in electron transfer experiments.<sup>7</sup>

Here, we carry out first-principles transport calculations on stable organic radicals<sup>8,9</sup> to test them for their properties as spin filters, i.e., as devices favoring transport of electrons with either spin up or spin down. We predict that the transport properties of benzene-based model radicals may differ to a sufficient extent for electrons of different spins to make them suitable candidates for such filters and that they may be tuned systematically by introducing additional substituents. Furthermore, the qualitative predictions made for our model systems are transferable to certain larger stable radicals.

As in previous work on electron tunneling through magnetic molecular systems,<sup>10</sup> we assume that correlations between tunneling electrons and the unpaired spins on the molecule play a minor role. There is both theoretical and experimental work on the importance of spin flips in tunneling processes.<sup>6,11</sup> Our analysis only holds for situations in which spin flips can be neglected, and it is not entirely clear yet to which molecules and conditions this applies.

This theoretical analysis of molecular transport properties in gold-molecule-gold junctions uses the Landauer–Imry approach<sup>12</sup> in combination with nonequilibrium Green's functions (NEGF)<sup>13</sup> and spin-unrestricted Kohn–Sham density functional theory (UKS-DFT).<sup>14</sup> This approach<sup>15</sup> relates the current  $I_s(V)$  for electrons of spin  $s \in \{\alpha, \beta\}$  to the transmission function  $T_s(E, V)$ , integrated over an energy ( $E$ ) interval which we take to be centered at the system's Fermi energy  $E_F$ , with a width determined by the symmetrically applied bias voltage  $V$ ,

$$I_s(V) = \frac{e}{h} \int_{E_F - \frac{eV}{2}}^{E_F + \frac{eV}{2}} dE T_s(E, V) \quad (1)$$

$e$  is the unit charge, and  $h$  Planck's constant. This relationship holds in the coherent tunneling regime, i.e., for low temperatures and short molecular bridges with a large separation between the one-particle energy levels and the Fermi energies of the electrodes ("off-resonant" conditions). Furthermore, the number of electrons on the molecule is assumed to be constant in time. The zero-voltage differential conductance may be estimated from the transmission at  $E_F$ . In the NEGF approach,  $T_s$  is calculated from a trace over matrices describing the coupling of a central region<sup>16</sup> to the left and right electrodes,  $\Gamma_{L,R,s}$ , and the central system subblock of the retarded and advanced Green's functions of the electrode-molecule-electrode system  $G_{C,s}^{r,a}$ .<sup>17</sup>

$$T_s(E, V) = \text{tr}(\Gamma_{R,s} G_{C,s}^r \Gamma_{L,s} G_{C,s}^a) \quad (2)$$

the advanced Green's function being the complex conjugate of the retarded.  $\Gamma_{X,s}$  and  $G_{C,s}^r$  are calculated from the overlap and Fock matrices of a finite-cluster electrode-molecule-electrode system,

$$\Gamma_{X,s} = -2\text{Im}[(ES_{XC} - H_{XC,s})^\dagger g_{X,s}(ES_{XC} - H_{XC,s})] \quad (3)$$

$$G_{C,s}^r = (ES_C - H_{C,s} + i\frac{1}{2}\Gamma_{R,s} + i\frac{1}{2}\Gamma_{L,s})^{-1} \quad (4)$$

The Fock and overlap matrices of the electrode-molecule-electrode system are divided into central, left-electrode, and right-electrode regions.  $S_{XC}$  and  $H_{XC,s}$  denote the coupling block of electrode  $X$  and molecule in the overlap and Fock matrix, respectively, while the molecule (or "central region") subblocks of these matrices are indicated by the subscript  $C$ . The Green's function matrices  $g_{X,s}$  of the isolated, infinite electrodes are described in the wide-band-limit approximation (see Supporting Information (SI)) and are not taken to be spin polarized. To construct the finite-cluster system, the structures of the dithiol molecules were optimized, the thiol hydrogen atoms were removed, and the molecules were placed between two  $\text{Au}_9$  clusters mimicking hollow site adsorption on  $\text{Au}(111)$  surfaces, with a sulfur–gold distance from a previous DFT

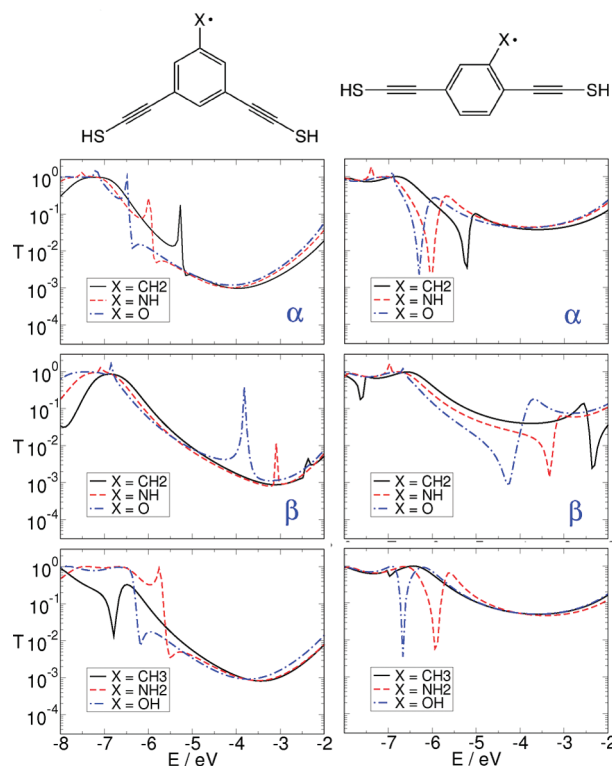


**Figure 1.**  $\alpha$  (majority spin) and  $\beta$  (minority spin) transmission calculated for *meta*- (left) and *para*-connected (right) model structures with various radical centers  $X$  in the doublet state. Closed-shell structures with an H atom added are given as a reference (bottom). B3LYP/LANL2DZ.

study.<sup>18</sup> In the self-consistent field algorithm, the density matrix was calculated assuming a closed system (see SI for further details).

For efficient spin filtering, the transmission for the two spin quantum numbers must differ appreciably over a sufficiently broad energy range near  $E_F$  to be experimentally observable. The two most pronounced types of features in the transmission which are useful for this purpose are peaks and dips. Peaks occur close to the molecular orbital (MO) energies obtained from solving the secular equation for the central region subblock of the one-particle Hamiltonian matrix. Since, for optimal spin filtering, these peaks need to be close to  $E_F$ , this would imply moving into the resonant tunneling regime, in which eq 1 is no longer a good approximation. Thus, the type of feature suited for designing spin filters within the Landauer regime are dips, which may be caused by destructive interference,<sup>19,20</sup> and which may occur far from any resonances (i.e., central subsystem MO (CMO) energies). Conduction properties may vary with the molecular conformation and with the way the molecules are adsorbed on the electrodes.<sup>21,22</sup> Therefore, it will be an important task for future studies to ensure that the trends observed for the minimum energy structures of the isolated dithiols are consistent over the full range of experimentally relevant structures. Prior studies on closed-shell systems with dominant dips near  $E_F$  have indicated that these features remain in the presence of structural variations likely at ambient temperature.<sup>22</sup>

Transmission curves have been calculated for benzene derivatives connected to gold electrodes, with  $sp^2$  hybridized  $\text{CH}_2$ ,  $\text{NH}$ , and  $\text{O}$  radical groups attached, modeling radical centers found in typical stable radicals.<sup>8,9</sup> The radicals are assumed to be in a doublet state, with the unpaired electron having an  $\alpha$  spin. Two modes of attachment to the electrodes are considered, with the unsubstituted closed-shell *meta*-connected benzene species known to have a much lower conductance than the *para*-connected one.<sup>19,23</sup> Figure 1 shows the transmission through the radical systems and their closed shell counterparts. Near  $E_F$  several features shift with the substituent and, in the radical systems, shift with spin projection. In the radical systems, these features are ordered systematically from high to low energies such that  $\text{CH}_2 > \text{NH} > \text{O}$ . For the *meta*-connected radicals, peaks are dominant, while their *para*-connected analogues show pronounced dips. This may be related to the transmission for the unsubstituted systems, i.e., the “baseline”, being higher for the *para* system. Except for the  $\text{X} = \text{O}$   $\beta$  transmission, the peaks in the *meta*-connected structures are less significant than the dips in the *para*-connected ones. The broadest dip is in the  $\beta$  transmission of the  $\text{X} = \text{O}$  structure, but this changes with the basis set or functional used (see SI). The dip is close to  $E_F$ ,  $-5.5$  eV<sup>24</sup> for bulk gold, making this a possible candidate for dominant  $\alpha$  (or majority spin) conductance.

The Fermi energy of bulk gold is a very rough estimate for  $E_F$  suitable for use in eq 1, when employed in combination with a finite-cluster approach involving only small electrode clusters and a minimal central region (the “band lineup problem”<sup>25</sup>). The approximations inherent in using small clusters, however, are expected to have a minimal impact on qualitative comparisons between different molecules, as long as the same set of approximations is used throughout. Once the location of  $E_F$  can be determined, for example, through sophisticated calculations involving very large electrodes,<sup>26</sup> this information could be transferred to other small-cluster calculations on similar molecules.

Since, in the Landauer approach, explicit interactions between electrons on the bridge and tunneling electrons are neglected, the transmission does not directly depend on MO occupations. It does so indirectly, of course, because the number of  $\alpha$  and  $\beta$  electrons will influence the CMO shapes and energies, which control the transmission. Differences between  $\alpha$  and  $\beta$  orbitals will thus lead to differences in transport. As can be seen in Figure 2 for the *para*-

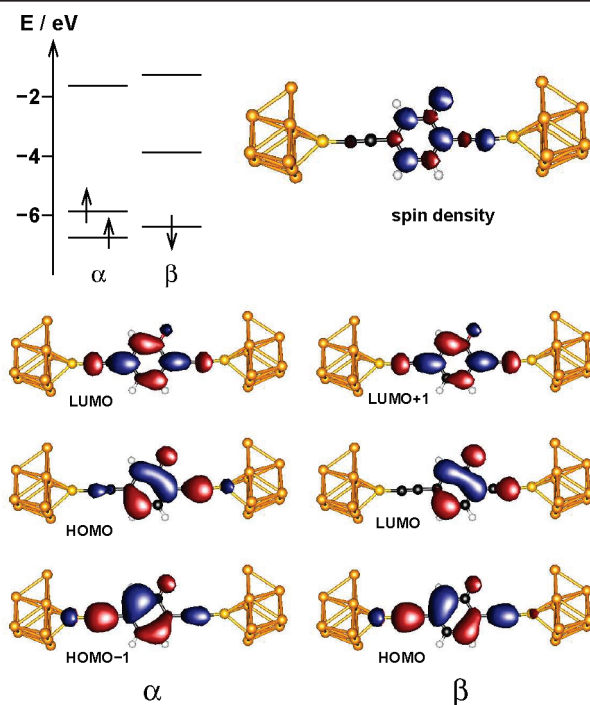


**Figure 2.** Central subsystem MO energies and isodensity plots of central subsystem system MOs and the total system’s spin density for the *para*-connected  $\text{X} = \text{O}$  radical. B3LYP/LANL2DZ.

connected  $\text{X} = \text{O}$  radical, the  $\alpha$  and  $\beta$  CMO shapes differ only a little, while the  $\beta$  CMOs are shifted to higher energies. This shift is most pronounced for the  $\text{HOMO}_\alpha/\text{LUMO}_\beta$  pair, and it corresponds to the features in the  $\beta$  transmission being qualitatively similar to the  $\alpha$  ones, but shifted to higher energies. Figure 2 also illustrates that the spin density is localized on the molecular bridge and does not “spill” onto the electrodes. It cannot be excluded, however, that this is an artifact of the approximate exchange-correlation functional.

To control spin transport properties, the ability to shift the features in the transmission is crucial. The peaks and dips reported here are due to the  $\pi$  orbital system (see SI), and interference features arising from the  $\pi$  orbitals have been shown to be highly amenable to energetic tuning by chemical substitution.<sup>27</sup> Indeed, when adding a nitro or amino substituent *ortho* to the radical group in the *para*-connected species (Figure 3), the dips are shifted by up to 1.5 eV to lower and higher energies, respectively. Where multiple dips are visible, the relevant ones were identified by comparing the energies and shapes of the CMOs of the substituted system with those of the unsubstituted system.

The model systems illustrate the interesting dual character that these spin filters can exhibit. Taking the transmission at the bulk gold Fermi energy of the  $\text{X} = \text{O}$  systems for example, it appears that the nitro substituent gives preferential transport of the  $\alpha$  spin component; however, with the amino substituent there will be preferential  $\beta$  spin transport. Thus, a system can be designed to filter either spin component, irrespective of the magnetization of the radical.

To check whether these conclusions can, in principle, be transferred to stable organic radicals, spin-resolved transmission curves for a *meta*-connected trityl radical and a *para*-connected dimer subunit of a stable ferromagnetic radical polymer<sup>8</sup> are displayed in Figure 4. For both species, the qualitative features of the corresponding model radicals ( $\text{X} = \text{CH}_2$  curve on the left-hand side and  $\text{X} = \text{O}$  curve on the right-hand side of Figure 1) are reproduced, although the peaks and dips tend to be more narrow.

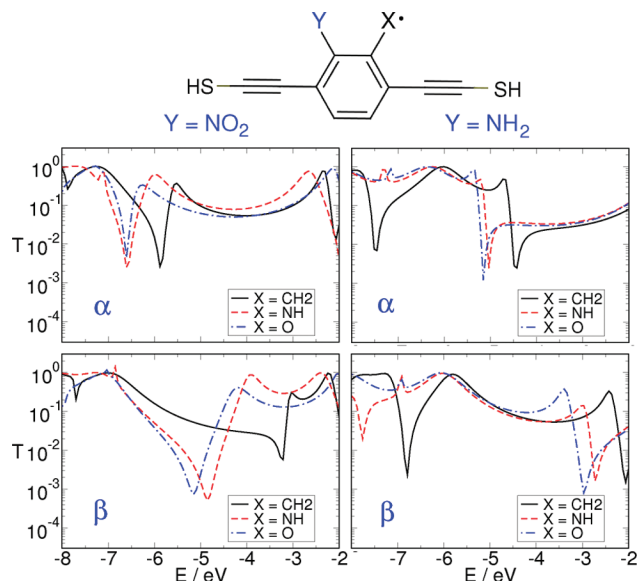


**Figure 3.**  $\alpha$  (majority spin) and  $\beta$  (minority spin) transmission calculated for the *para*-connected model structures in the doublet state with one additional substituent Y ortho to the radical group X. B3LYP/LANL2DZ.

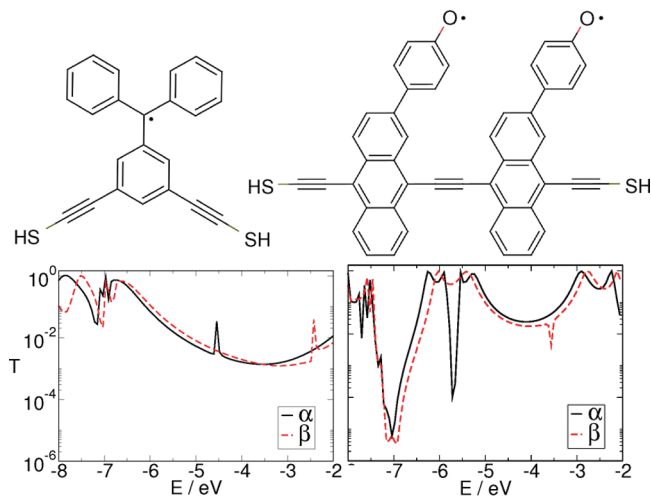


**Figure 4.**  $\alpha$  (majority spin) and  $\beta$  (minority spin) transmission calculated for a *meta*-connected trityl singlet radical (left) and a *para*-connected triplet dimer of a stable ferromagnetic radical polymer.<sup>8</sup> B3LYP/LANL2DZ.

It may be anticipated that, in actual devices, the radicals will not necessarily be sandwiched between two electrodes as assumed here. Instead they might, for example, serve as magnetic building blocks combined in a ferromagnetically or antiferromagnetically coupled way and thus control the overall charge transport properties. Alternatively, they may act as bridges which mediate electronic communication to a different extent for electrons of different spin. From a conceptual point of view, the results discussed here may nonetheless be relevant for these scenarios, and further studies on chemical tuning of stable organic radicals might lead to interesting test systems for experimental investigations of their conduction properties. Such experiments, as well as further theoretical work, might also help to elucidate the types of systems and experimental conditions under which spin flip scattering plays an important role.

**Acknowledgment.** We thank J. Subotnik for a customized version of Qchem and V. Mujica, H. Baranger, and M. di Ventra for helpful discussions. C.H. gratefully acknowledges funding through a Forschungsstipendium by the Deutsche Forschungsge-

meinschaft (DFG). This material is based upon work supported as part of the NERC, an Energy Frontier Research Center funded by the U.S. Department of Energy, Office of Science, Office of Basic Energy Sciences under Award Number DE-SC0000989.

**Supporting Information Available:** Details on the computational methodology; results for different density functionals, basis sets, substitution patterns, and linkers; spin-resolved current and conductance; MO analysis; spin and charge state energetics; Hückel and symmetry analysis for closed-shell systems; molecular coordinates and energies. This material is available free of charge via the Internet at <http://pubs.acs.org>.

## References

- (1) (a) Nitzan, A.; Ratner, M. A. *Science* **2003**, *300*, 1384–1389. (b) Tao, N. J. *Nat. Nanotechnol.* **2006**, *1*, 173–181. (c) Joachim, C.; Ratner, M. A. *Proc. Natl. Acad. Sci. U.S.A.* **2005**, *102*, 8801–8808. (d) Di Ventra, M. *Electrical Transport in Nanoscale Systems*; Cambridge University Press: Cambridge, 2008.
- (2) Aviram, A.; Ratner, M. *Chem. Phys. Lett.* **1974**, *29*, 277–283.
- (3) (a) Žutić, I.; Fabian, J.; Sarma, S. D. *Rev. Mod. Phys.* **2004**, *76*, 323–410. (b) Wolf, S. A.; Chitchelekanova, A. Y.; Treger, D. M. *IBM J. Res. Dev.* **2006**, *50*, 101–110. (c) Seneor, P.; Bernard-Mantel, A.; Petroff, F. J. *Phys.: Condens. Matter* **2007**, *19*, 165222.
- (4) Wang, F.; Vardeny, Z. V. *J. Mater. Chem.* **2009**, *19*, 1685–1690.
- (5) Sanvito, S. *J. Mater. Chem.* **2007**, *17*, 4455–4459.
- (6) Sugawara, T.; Minamoto, M.; Matsushita, M. M.; Nickels, P.; Komiyama, S. *Phys. Rev. B* **2008**, *77*, 235316.
- (7) Chernick, E. T.; Mi, Q.; Vega, A. M.; Lockard, J. V.; Ratner, M. A.; Wasielewski, M. R. *J. Phys. Chem. B* **2007**, *111*, 6728–6737.
- (8) Kaneko, T.; Matsubara, T.; Aoki, T. *Chem. Mater.* **2002**, *14*, 3898–3906.
- (9) Rajca, A.; Shiraishi, K.; Pink, M.; Rajca, S. *J. Am. Chem. Soc.* **2007**, *129*, 7232–7233.
- (10) (a) Tagami, K.; Tsukada, M. *J. Phys. Chem. B* **2004**, *108*, 6441–6444. (b) Chen, Y.; Prociuk, A.; Perrine, T.; Dunietz, B. D. *Phys. Rev. B* **2006**, *74*, 245320. (c) Perrine, T. M.; Dunietz, B. D. *J. Phys. Chem. A* **2008**, *112*, 2043–2048. (d) Liu, R.; Ke, S.-H.; Yang, W.; Baranger, H. U. *J. Chem. Phys.* **2007**, *127*, 141104. (e) Liu, R.; Ke, S.-H.; Baranger, H. U.; Yang, W. *Nano Lett.* **2005**, *5*, 1959–1962.
- (11) (a) Krause, S.; Berbil-Bautista, L.; Herzog, G.; Bode, M.; Wiesendanger, R. *Science* **2007**, *317*, 1537–1540. (b) Lorente, N.; Gauyacq, J.-P. *Phys. Rev. Lett.* **2009**, *103*, 176601.
- (12) (a) Landauer, R. *IBM J. Res. Dev.* **1957**, *1*, 223–231. (b) Büttiker, M.; Imry, Y.; Landauer, R.; Pinhas, S. *Phys. Rev. B* **1985**, *31*, 6207–6215.
- (13) Mahan, G. D. *Many-particle Physics*; Plenum Press: New York, 1990.
- (14) (a) Kohn, W.; Sham, L. J. *Phys. Rev.* **1965**, *140*, 1133–1138. (b) Hohenberg, P.; Kohn, W. *Phys. Rev.* **1964**, *136*, 864–871.
- (15) Due to issues such as an uncertain Fermi energy, the inadequacy of KS MOs to describe transport through many-electron systems, and the approximate nature of the available exchange-correlation functionals, this approach should not, in general, provide quantitative accuracy. However, it is a very valuable tool for qualitative predictions and analyses.
- (16) Here, the central region contains the molecule only, although frequently electrode atoms are included for improved quantitative accuracy.
- (17) (a) Caroli, C.; Combescot, R.; Nozières, P.; Saint-James, D. *J. Phys. C: Solid State Phys.* **1971**, *4*, 916–929. (b) Meir, Y.; Wingreen, N. S. *Phys. Rev. Lett.* **1992**, *68*, 2512–2516.
- (18) Bilić, A.; Reimers, J. R.; Hush, N. S. *J. Chem. Phys.* **2005**, *122*, 094708.
- (19) (a) Sautet, P.; Joachim, C. *Chem. Phys. Lett.* **1988**, *153*, 511–516. (b) Patoux, C.; Couderc, C.; Launay, J.-P.; Joachim, C.; Gourdon, A. *Inorg. Chem.* **1997**, *36*, 5037–5049. (c) Onuchic, J. N.; Beratan, D. N.; Winkler, J. R.; Gray, H. B. *Annu. Rev. Biophys. Biomol. Struct.* **1992**, *21*, 349–377.
- (20) (a) Ke, S.-H.; Yang, W.; Baranger, H. U. *Nano Lett.* **2008**, *8*, 3257–3261. (b) Solomon, G. C.; Andrews, D. Q.; Hansen, T.; Goldsmith, R. H.; Wasielewski, M. R.; Van Duyne, R. P.; Ratner, M. A. *J. Chem. Phys.* **2008**, *129*, 054701.
- (21) (a) Reichert, J.; Ochs, R.; Beckmann, D.; Weber, H. B.; Mayor, M.; Löhneysen, H. v. *Phys. Rev. Lett.* **2002**, *88*, 176804. (b) Smit, R. H. M.; Noat, Y.; Untiedt, C.; Lang, N. D.; van Hemert, M. C.; van Ruitenbeek, J. M. *Nature* **2002**, *419*, 906–909. (c) Xu, B.; Tao, N. J. *Science* **2003**, *301*, 1221–1223. (d) Venkataraman, L.; Klare, J. E.; Tam, I. W.; Nuckolls, C.; Hybertsen, M. S.; Steigerwald, M. L. *Nano Lett.* **2006**, *6*, 458–462.
- (22) Andrews, D. Q.; Solomon, G. C.; Goldsmith, R. H.; Hansen, T.; Wasielewski, M. R.; Van Duyne, R. P.; Ratner, M. A. *J. Phys. Chem. C* **2008**, *112*, 16991–16998.
- (23) Mayor, M.; Weber, H. B.; Reichert, J.; Elbing, M.; von Hänisch, C.; Beckmann, D.; Fischer, M. *Angew. Chem., Int. Ed.* **2003**, *42*, 5834–5838.
- (24) Ashcroft, N. W.; Mermin, N. D. *Solid State Physics*; Holt Rinehart & Winston: Austin, 1976.
- (25) Xue, Y.; Datta, S.; Ratner, M. A. *J. Chem. Phys.* **2001**, *115*, 4292–4299.
- (26) Pauly, F.; Viljas, J. K.; Cuevas, J. C.; Schön, G. *Phys. Rev. B* **2008**, *77*, 155312.
- (27) Andrews, D. Q.; Solomon, G. C.; Van Duyne, R. P.; Ratner, M. A. *J. Am. Chem. Soc.* **2008**, *130*, 17309–17319.

JA910483B